Transonic Airfoil Flow Simulation.
Part I: Mesh Generation and Inviscid Method

Florin FRUNZULICĂ[*,**], Horia DUMITRESCU[**], Alexandru DUMITRACHE[**], Vladimir CARDOS[**]

*Corresponding author
[*]Department of Aerospace Engineering, "POLITEHNICA"
University of Bucharest, 1 Gh.Polizu Street, Sect.1, Romania
ffrunzi@yahoo.com
[**]Institute of Mathematical Statistics and Applied Mathematics
13 September Street, Sect. 5, Bucharest, Romania
alex_dumitrache@yahoo.com

Abstract: A calculation method for the subsonic and transonic viscous flow over airfoil using the displacement surface concept is described. Part I presents a mesh generation method for computational grid and a finite volume method for the time-dependent Euler equations. The inviscid solution is used for the inviscid-viscous coupling procedure presented in the Part II.

Key Words: transonic flow, mesh generation, Euler equations.

1. INTRODUCTION

In the last years transonic flow about airfoils has become a large range of interest. While transonic airfoil design plays an important role in the efficiency of the commercial present day airplanes, the increase in transonic manoeuvre limits of fighter aircraft with transonic wing design has been proved in flight tests for various prototypes. This transonic wing technology is nearly in all based on the availability of calculation methods for design and analysis in transonic flow since the wind tunnels are limited in Reynolds number and the cost of experiments in some cases can be prohibitive. On the other hand, in transonic flows the viscous effects strongly affect the performance of airfoils, so that the calculation methods for viscous transonic flow are particularly important.

The transonic regime is analyzed with solvers based on the Reynolds Averaged Navier-Stokes model [1-4] or solvers based on the viscous-inviscid interaction methods [5-9].

The present approach consists of the iterative application of an unsteady finite-volume Euler method and a boundary layer part with semi-empirical models for separated regions using the displacement thickness concept. The inviscid flow method is discussed first (Part I), followed by a description of the integral boundary-layer methods (Part II). The methods used to couple the viscid-invicid solutions is described, followed by computed results for supercritical flows over some airfoils for which experimental surface pressure and boundary/layer data are available.

2. CALCULATION METHOD

2.1 Mesh Generation

The method used for mesh generation is based on the free form deformation (FFD) and it has

origin in „linear/ nonlinear analysis" of structures.

The generating principle is simple: knowing the final state of deformation of the domain boundaries, the real problem is to determine the forces that lead to obtaining a certain deformed structure. Formally, the problem may be written as:

$$\begin{bmatrix} \mathbf{K}_{11} & \mathbf{K}_{12} \\ \mathbf{K}_{21} & \mathbf{K}_{22} \end{bmatrix} \cdot \begin{Bmatrix} \boldsymbol{\delta}_n \\ \boldsymbol{\delta}_c \end{Bmatrix} = \begin{Bmatrix} \mathbf{0} \\ \mathbf{F}_a \end{Bmatrix} \Leftrightarrow \begin{cases} \mathbf{K}_{11} \cdot \boldsymbol{\delta}_n + \mathbf{K}_{12} \cdot \boldsymbol{\delta}_c = \mathbf{0} \\ \mathbf{K}_{21} \cdot \boldsymbol{\delta}_n + \mathbf{K}_{22} \cdot \boldsymbol{\delta}_c = \mathbf{F}_a \end{cases} \quad (1)$$

where: $\mathbf{K}$ represents the structure stiffness matrix, $\boldsymbol{\delta}$ displacement vector which contains $\boldsymbol{\delta}_n$ - the unknown displacements of the interior nodes and $\boldsymbol{\delta}_c$ the known displacements of the boundaries.

The vector of forces, $\mathbf{F}$, may also be divided into two sub-components: a sub-vector $\mathbf{0}$, which corresponds to the interior nodes of the structure and a sub-vector of the forces (unknown yet), $\mathbf{F}_a$, which creates the structure deformation (these forces will act on the domain boundaries). We will not insist on determining the stiffness matrix for constitutive elements $\mathbf{K}_e$, the assembling mode of the elementary stiffness matrix and the solving procedures of the resulting linear equations system, because these are presented in detail in any book dedicated to analysis of structures with the finite element method [10]. It is not necessary that all the nodal displacements on the boundaries to be known; additional conditions may be required for the nodes which are supposed to glide on boundaries.

The first equation of the divided system (1) will give us the unknown displacements:

$$\boldsymbol{\delta}_n = -\mathbf{K}_{11}^{-1} \cdot \mathbf{K}_{12} \cdot \boldsymbol{\delta}_c \quad (2)$$

and the last equation

$$\mathbf{F}_a = \mathbf{K}_{21} \cdot \boldsymbol{\delta}_n + \mathbf{K}_{22} \cdot \boldsymbol{\delta}_c \quad (3)$$

will give the applied forces $\mathbf{F}_a$ that create the supposed pattern of deformation field.

The determination of new positions of interior nodes can be realized also by solving the global problem:

$$\mathbf{K} \cdot \boldsymbol{\delta} = \mathbf{F} \quad (4)$$

The deformation process generates a re-arrangement of the interior nodes of the mesh. The main advantage is the preserving of a quasi-regularity of mesh near the boundaries.

Passing from the initial mesh to the final mesh may assume large deformations of the domain frontier. In that situation, in order to keep the small deformations hypothesis, is necessary to consider a step-by-step deformation of the structure, which will be made in several stages, without taking into account the remanent strain state of the previous step.

The mesh generation control can be done by allowing the elastic characteristics of structure (E, ν) to variate in the computational domain; there is no physical support between those characteristics and the existing materials (we have a fictitious material).

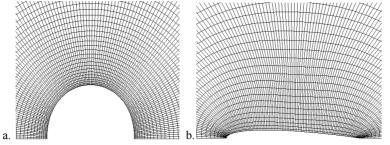In Figure 1 is presented a mesh, before deformation (a) and after deformation (b).

Fig. 1 – Initial mesh (a) and (b) mesh after deformation process

2.2 Inviscid Method

The two-dimensional unsteady Euler equations are written in the conservative form as

$$\frac{\partial U}{\partial t} + \nabla \vec{F} = 0 \tag{5}$$

where

$$U = \left\{ \rho \quad \rho u \quad \rho v \quad \rho E \right\}^T$$
$$\vec{F} = f \cdot \vec{i} + g \cdot \vec{j} \tag{6}$$

$$f = \left\{ \rho u \quad \rho u^2 + p \quad \rho uv \quad (\rho E + p)u \right\}^T$$
$$g = \left\{ \rho v \quad \rho uv \quad \rho v^2 + p \quad (\rho E + p)v \right\}^T \tag{7}$$

and

$$E = \frac{1}{2}\left(u^2 + v^2\right) + \frac{1}{\gamma - 1}\frac{p}{\rho} \tag{8}$$

for a perfect gas.

For the conservative variables (**U**), the integral formulation of Eq.(5) is given by

$$\frac{\partial}{\partial t} \int_{\sigma_e} U \, d\sigma + \int_{\partial \sigma_e} \left(f(U) n_x + g(U) n_y \right) ds = 0 \tag{9}$$

where $\vec{n} = n_x \vec{i} + n_y \vec{j}$ is the outward normal of the element boundary $\partial \sigma_e$. In this form, is attractive to use a Finite Volume Method (FVM), especially for the case of the convective dominant flows.

The main feature of the FVM is the integration of the flux on the surface of the control volume σ_e. For the convective terms, the problem becomes 1-D in the direction of the normal to the surface. The one-dimensional Euler system may be easily diagonalized and then the surface flux can be evaluated in an upwind purpose.

In order to perform calculations on the structured meshes, changing the cartesian coordinates with coordinates attached to the local directions of structured mesh is justified:

$$\xi = \xi(x, y), \eta = \eta(x, y) \tag{10}$$

where ξ is the coordinate along airfoil surface and η is the normal coordinate to airfoil.

Using the geometric transformation (10), having the Jacobian (11) and the variables (12)

$$J = \frac{\partial(\xi, \eta)}{\partial(x, y)} \tag{11}$$

$$\tilde{U} = U / J \tag{12}$$

eq. (9) becomes

$$\frac{\partial \tilde{U}}{\partial t} + \frac{\partial \tilde{f}(\tilde{U})}{\partial \xi} + \frac{\partial \tilde{g}(\tilde{U})}{\partial \eta} = 0 \tag{13}$$

where the flux components f and g are given by:

$$\tilde{f} = \frac{1}{J}\nabla \xi \cdot \vec{F}(U) \, , \, \tilde{g} = \frac{1}{J}\nabla \eta \cdot \vec{F}(U) \tag{14}$$

$\bar{U}$ denote the medium state on the cell and U represents the vector of conservative variables.

The contravariant velocities have the following form:

$$u_\xi = \nabla \xi \cdot \vec{V} \ , \ v_\eta = \nabla \eta \cdot \vec{V} \tag{15}$$

We had used the cell-centered finite volume for the spatial approximation of solution. For each cell (i , j) results the differential equation:

$$\sigma_{i,j} \frac{\partial \bar{U}_{i,j}(t)}{\partial t} + \left(\tilde{f}_{i+1/2,j} - \tilde{f}_{i-1/2,j} \right) + \left(\tilde{g}_{i,j+1/2} - \tilde{g}_{i,j-1/2} \right) = 0 \tag{16}$$

where the numerical fluxes $\tilde{f}_{i+1/2}, \tilde{f}_{i-1/2,j}$, etc. contain both the outwards normal and the boundary length of the element, because $\left(\nabla \xi / J \right)_{i+1/2,j} = \left(\vec{n}_\xi s \right)_{i+1/2,j}$, etc. The fluxes are calculated in upwind manner with left/right states of the adjacent cells. For example, the flux through $(i+1/2, j)$ interface is given by

$$\tilde{f}_{i+1/2,j} = \int_{s_{1+1/2}} F_s \left(U_{i,j}(t), U_{i+1,j}(t), \vec{n}_{i+1/2,j} \right) ds$$
$$\cong s_{i+1/2} F_\sigma \left(U_{i,j}(t), U_{i+1,j}(t), \vec{n}_{i+1/2,j} \right) \tag{17}$$

and it is calculated numerically using the Roe scheme [11]. This scheme is simple and efficiently, and is strict connected with the hyperbolic character of the Euler system.

The time integration with the fourth order Runge-Kutta scheme is already classic scheme for the discretization with FVM. The evolution in time is referred at the medium state corresponding to each finite volume cell. Therefore, we have implemented the scheme proposed by Jameson [12], which consists in the following steps:

$$U_e^{(0)} = \bar{U}_e(t_n) = \bar{U}_e^n$$
$$\bar{U}_e^{(p)} = \bar{U}_e^{(0)} + \alpha_p \Delta t \, R_e \left(\bar{U}^{(p-1)} \right), p = 1...m \tag{18}$$
$$\bar{U}_e^{(n+1)} = \bar{U}_e^{(m)}$$

where the coefficients α_p are given by

$$\alpha_p = \frac{1}{m - p + 1}, \ p = 1...m$$

The global step time is chosen following the well-know stability criterion [13]:

$$\Delta t = \min_k \left(CFL \cdot \frac{l_k}{|\vec{V}_k \vec{n}_k| + \bar{c}_k} \right)$$

which ensures that the simple wave produced at the cell interface should not pass over the boundaries of the neighbouring cells.

Boundary condition is ruled by the type of the boundaries and the hyperbolic character of the Euler system.

The infinite boundary (in the case of exterior flows) is a fictive boundary which limits the computational domain. We had supposed that the fluid state remains unchanged outside of the computational domain. Thus, the calculus of fluxes is performed using the neighbouring cells of the fluid boundary and a fictive cell outside of the computational domain.

At the wall, for inviscid flows, the boundary condition is:

$$\vec{V} \cdot \vec{n} = 0 \tag{19}$$

and as a consequence the convective flux vanishes.

This condition is implemented using a fictive cell on the solid frontier where the velocity has the opposite sign with respect to the velocity in the neighbouring cell, while pressure, density and energy remain constant. A numerical correction for the interior component of velocity is required:

$$\vec{V} = \vec{V}_c - \left(\vec{V}_c \vec{n} \right) \vec{n} \tag{20}$$

where $\vec{V}_c$ is the calculate velocity.

To obtain the second order spatial accuracy, we have adopted a MUSCL formulation (Monotone Upstream-centred Schemes for Conservation Laws) for nonuniform structured grid. The limiter used in MUSCL reconstruction (at the interface level) was proposed by van Albada [13], because it has simple mathematical form and smooth properties.

3. RESULTS AND DISCUSSION

The results presented here have been obtained using a computational "C" grid with 280x75 points (Fig. 2). The solution was obtained with a residual of 10^{-6} in the inviscid part and it was used for interacting cycle in inviscid-viscous method.

We start with some calculations for the RAE 2822 airfoil. In [14] a number of cases have been extensively tested. We have chosen the case: $M_\infty = 0.725$, $Re = 6.5 \cdot 10^6$, $\alpha_{exp} = 2.3^0$, transition point at 3%.

Figure 3 shows a comparison of the pressure coefficient distribution calculated without boundary layer and experiment.

The agreement between computational solution and experiment is relatively good in limit of inviscid flow assumptions.
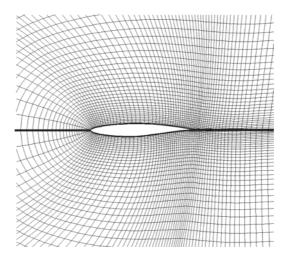

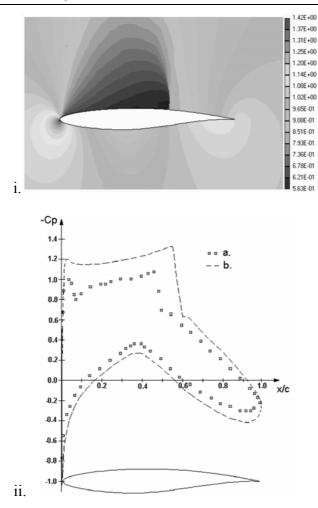Fig. 2 – C-grid (280 x 75 points) obtained using free form deformation

Fig. 3 – Pressure coefficient isolines (i) and distribution (ii) for the RAE2822 airfoil: $M_\infty = 0.725$,

$\mathrm{Re} = 6.5 \cdot 10^6$, $\alpha_{\exp} = 2.3^0$: (a) experiment, (b) inviscid solution (Euler).

The present work will be continued with Part II including the inviscid − viscous interaction method.

REFERENCES

[1] T.L Holst, U. Kaynak, K.L. Grundy, Transonic wing flows using an Euler/Navier-Stokes zonal approach., *Journal of Aircraft*, vol. **24**, no.1, pp 17-24, 1987.

[2] A. Jameson, N.A. Pierce and L. Martinelli, Optimum aerodynamic design using the Navier-Stokes equations, *AIAA Paper* 97-0101, Jan 1997.

[3] M. Jayaram and A. Jameson, Multigrid solution of Navier-Stokes equations for flow over wings, *AIAA Paper* 88-0705, Jan 1988.

[4] D. Mavriplis and A. Jameson, Multigrid solution of the Navier-Stokes equations on triangular meshes, *AIAA Journal*, vol. **28**, pp. 1415-1425, 1990.

[5] R.C. Lock and B.R Williams, Viscous-inviscid interactions in external aerodynamics, *Progress Aerospace Sciences*, vol. **24**, pp 51-171, 1987.

[6] R.E. Melnik, R.R. Chow, H.R. Mead and A. Jameson, An inproved viscid/inviscid interaction procedure for transonic flow over airfoils, *NASA CR*-3805, Oct 1985.

[7] W. Schmidt, A. Jameson and D.D. Whitfield, Finite volume solutions for the Euler equations for transonic flow over airfoils and wings including viscous effects, *AIAA Paper* 81-1265, 1981.

[8] M. Drela and B.B. Giles, Viscous-inviscid analysis of transonic and low Reynolds number airfoils, *AIAA Journal*, vol. **25**, pp.1347-1355, 1987.

[9] D.P. Coiro, M. Amato and P. De Matteis, Numerical predictions of transonic viscous flows around airfoils through an Euler/boundary layer interaction method, *Aeronautical Journal*, pp.157-165, April, 1992.

[10] O.C. Zienkiewicz, R.L. Taylor, *The Finite Element Method*, 4 th edn, vols 1,2, McGraw-Hill, New-York, 1989.

[11] P.L. Roe, Approximated Riemann Solvers. Parameter Vectors and Difference Scheme, *J. Comput. Phys.*, vol. 43 pp. 357-372, 1981.

[12] A. Jameson, Numerical Simulation of the Euler Equations by Finite Volume Methods Using Runge-Kutta Steping Schemes, *AIAA paper* 81-1259, 1981.

[13] Van Albada, B. Van Leer, W.W. Roberts, A comparative study of computational methods in cosmic gas dynamics, *Astron. Astrophysics*, vol. **108**, pp 76-84, 1982.

[14] P.H. Cook, M.A. McDonald and M.C.F. Formin, Airfoil RAE 2822 pressure distribution and boundary layer measurements, *AGARD-AR*-138 /1979.